Multicolor XUV above threshold ionization of argon

2015 J. Phys. B: At. Mol. Opt. Phys. 48 245202

(http://iopscience.iop.org/0953-4075/48/24/245202)

IOP Publishing Journal of Physics B: Atomic, Molecular and Optical Physics
J. Phys. B: At. Mol. Opt. Phys. **48** (2015) 245202 (9pp) doi:10.1088/0953-4075/48/24/245202

Multicolor XUV above threshold ionization of argon

R Della Picca[1] **and E Lindroth**[2]

[1] CONICET and Centro Atómico Bariloche, Av. Bustillo 9500, 8400 Bariloche, Argentina
[2] Department of Physics, Stockholm University, Alba Nova University Center, SE-106 91 Stockholm, Sweden

E-mail: renata@cab.cnea.gov.ar

Received 1 July 2015
Accepted for publication 2 September 2015
Published 23 October 2015

Abstract

Argon photo-electron spectra produced by short-pulse extreme ultraviolet radiation, and with particular emphasis on the two-photon absorption region, is analyzed theoretically. The electromagnetic pulse is modeled to resemble experimentally available pulses and is built from a range of high-harmonics from an 800 nm laser. The photo-electron spectra show a characteristic peak structure due to the absorption of different combinations of photons, where the relative peak intensity is very sensitive to both the XUV pulse parameters and the target description. The theoretical result is further compared with experimental data, and good qualitative agreement is found.

Keywords: ATI, argon, XUV, laser ionization, two-photon ionization

(Some figures may appear in colour only in the online journal)

1. Introduction

Techniques based on the process of high harmonic generation (HHG) have led to the strong development of attosecond metrology, which has taken place during the last decade and opened up the field of electron dynamics in atomic and molecular processes for studies in the time domain [1]. The dominating techniques here use the extreme ultraviolet (XUV) pulses (or pulse-trains) generated when atoms interact with a strong laser field, and take advantage of the inherent synchronization with this laser field to obtain temporal information. In these XUV-IR pump and probe schemes the laser field is often strong, while the XUV-field is generally weak. The dominating quantum process involved is then multi-photon absorption where one photon is of XUV energy, while the others are in the IR domain. When the IR-field is truly strong it significantly perturbs the studied system, which complicates the analysis of experiments. This is one reason for the drive to perform XUV-pump and XUV-probe studies. Another reason is the prospect of higher time resolution. However, XUV-pump and XUV-probe scenarios require short wavelength pulses strong enough to induce nonlinear processes. One route taken to achieve this is the use of harmonic generation from higher density targets than that achievable with gases [2–4].

In a recent paper Heissler *et al* [4] used the technique from [2] and was able to present energy-resolved photo electron spectra from the nonresonant two-XUV-photon ionization of argon. The XUV radiation used in the experiment in [4] consists of higher-order harmonics (11th to 16th) of the original laser ω_0 ($\lambda = 800$ nm) generated by the so-called relativistic oscillating mirror (ROM) process [2] from laser plasma interaction, and the photoelectron (PE) spectrum shows nicely the above-threshold ionization (ATI) peaks corresponding to different combinations of two harmonic photons. Here we combine an accurate many-body account of the target atom with a field-dressed description of the photo electron, also accounting for the interaction with the residual ion, to address this scenario theoretically.

The theoretical description of a few-cycle pulse interacting with atoms is often obtained neglecting the multi-electronic nature of the target. This is true even when the calculations are based on the numerical solution of the time-dependent Schrödinger equation, with the exception of truly small systems where large scale calculations have been performed on Helium [5–10] and H_2 [11], for example. The commonly used strong field approximation (SFA) neglects

even the interaction of the emitted electron with the residual target ion [12]. A relatively cheap method that accounts for this latter interaction is the Coulomb–Volkov approach (CV) [13], but the ionization process is still mostly considered in the single active electron approximation which neglects many-body effects. From numerous studies of single photon ionization it is, however, well known that atom-specific effects often play a significant role. Argon, for example, has a strong so-called Cooper minimum for photon energies of around 50 eV. This is due to the vanishing overlap between the bound state wave function and that of the continuum, and the strong variation of one-photon absorption in this region is likely to modify the multi-photon signal as well. A good description of the position of the Cooper minimum requires not only a correct account for the Coulomb interaction in the final state, but also a certain amount of many-body effects. These requirements are fulfilled with the so-called random phase approximation with exchange (RPAE), as shown already in the eighties [14]. Here we combine the RPAE approach with the Coulomb–Volkov treatment of the above threshold ionization, which can be further approximated due to the properties of the light-field considered. This is detailed in section 2. We try to use approximately the same light-pulse parameters as in the experiment by Heissler *et al* [4] and find good qualitative agreement. Some of these results were also discussed in our previous work [15]. In section 3 we compare the spectra obtained with different approaches, and analyze the sensitivity to different parameters, concluding that the two-photon absorption energy region is very sensitive to the target description and the delay between the harmonics.

Atomic units are used, except when otherwise stated.

2. Theory

2.1. The Coulomb–Volkov approximation

In this section we summarize the Coulomb–Volkov (CV) approach and discuss the different additional approximations that will be employed here. A more detailed description can be found in [16]. The Coulomb–Volkov transition matrix in the length gauge reads [13]:

$$T_{fi} = -\mathrm{i}\int_0^\tau \left\langle \Psi_f^-(t)\middle|\boldsymbol{F}(t)\cdot\boldsymbol{r}\middle|\phi_i(t)\right\rangle \mathrm{d}t, \tag{1}$$

where $\phi_i(t)$ is the initial state target wave function with energy E_i in the absence of external fields, and Ψ_f^- is the CV wave function for the final electronic state that is the product of the ejected electron-target wave-function with ingoing boundary conditions and the Volkov phase:

$$\Psi_f^-(t) = \phi_f^-(\boldsymbol{r},\boldsymbol{k})\exp[-\mathrm{i}(S(\boldsymbol{k},t) - \boldsymbol{A}(t)\cdot\boldsymbol{r} + Et)], \tag{2}$$

where the length gauge Volkov phase is the quantity $[S - \boldsymbol{A}\cdot\boldsymbol{r}]$, with S defined by:

$$S(\boldsymbol{k},t) = \boldsymbol{k}\int^t \boldsymbol{A}(t')\mathrm{d}t' + \frac{1}{2}\int^t A^2(t')\mathrm{d}t'.$$

The ejected electron has momentum $\boldsymbol{k} \equiv (k, \Omega_k)$ corresponding to an energy of $E = \hbar^2k^2/2$.

The vector potential is obtained from the electric field of the ionizing radiation pulse as:

$$\boldsymbol{A}(t) = -\int^t \boldsymbol{F}(t')\mathrm{d}t'.$$

The differential ionization probability in energy is obtained from the transition matrix magnitude as

$$\frac{\mathrm{d}P^{CV}}{\mathrm{d}\,\mathrm{E}} = k\int \mathrm{d}\Omega_k \left|T_{fi}\right|^2. \tag{3}$$

The spatial dependence of the exponent of equation (2) is due to the term $i\boldsymbol{A}(t)\cdot\boldsymbol{r}$ only, and as discussed in [16] it can, when weak fields are considered, be handled through a series expansion [16]. The authors of [16] investigated the first few terms in this series. The first term with $\exp(i\boldsymbol{A}(t)\cdot\boldsymbol{r}) \approx 1$, is called the *DipA*-approximation, where it was found that it reproduced well the one-photon peak, and qualitatively the lower ATI peaks, for field-parameters close to what will be considered here. This is further discussed in section 3.1 below.

If the $\boldsymbol{A}(t)\cdot\boldsymbol{r}$ term is neglected, space and time are decoupled in the transition integrals, cf equation (1), and the transition matrix can be written as the product:

$$T \simeq \boldsymbol{L}(\boldsymbol{k})\cdot\boldsymbol{M}(\boldsymbol{k}) \tag{4}$$

where the contribution that accounts for the effect of the electromagnetic field on the free-electron final state is:

$$\boldsymbol{M}(\boldsymbol{k}) = \int_0^\tau \boldsymbol{F}(t)\,\mathrm{e}^{\mathrm{i}S(\boldsymbol{k},t)}\,\mathrm{e}^{\mathrm{i}\omega_{fi}t}\,\mathrm{d}t \tag{5}$$

with $\omega_{fi} = E - E_i$, while the factor $\boldsymbol{L} = \langle\varphi_f^-|\boldsymbol{r}|\varphi_i\rangle$ depends only on the target structure. This factor is the same as the one involved in the one-photon ionization cross section σ^{Ph}. The relation between $\boldsymbol{L}$ and σ^{Ph} is (see for example [17]):

$$\frac{\mathrm{d}\sigma^{Ph}}{\mathrm{d}\Omega_k\mathrm{d}E} = (2\pi)^2\alpha\Omega k\,|\boldsymbol{L}|^2\,\delta(E - E_i - \hbar\Omega) \tag{6}$$

for the absorption of one photon with frequency Ω. Here $\alpha \approx 1/137$ is the fine structure constant and the ejected electron energy is fixed by energy conservation. Often, the cross section is known, or can be accurately calculated, since it is independent of the characteristics of the electromagnetic field, and from equations (3)–(4) we can now get an approximate value for the multiphoton spectrum:

$$\begin{aligned}\frac{\mathrm{d}P^{DipA}}{\mathrm{d}\,\mathrm{E}} &= k\int \mathrm{d}\Omega_k\,|\boldsymbol{L}(\boldsymbol{k})|^2\,|\boldsymbol{M}(\boldsymbol{k})|^2 \\ &= \frac{(2\pi)^{-2}}{\alpha\omega_{fi}}\int \mathrm{d}\Omega_k\,|\boldsymbol{M}(\boldsymbol{k})|^2\,\frac{\mathrm{d}\sigma^{Ph}}{\mathrm{d}\Omega_k}\bigg|_{\Omega=\omega_{fi}},\end{aligned} \tag{7}$$

where we have put $\Omega = \omega_{fi}$.

Both terms inside the integral in equation (7) depend on the electron momentum, however an additional approximation can be made to achieve total decoupling, this

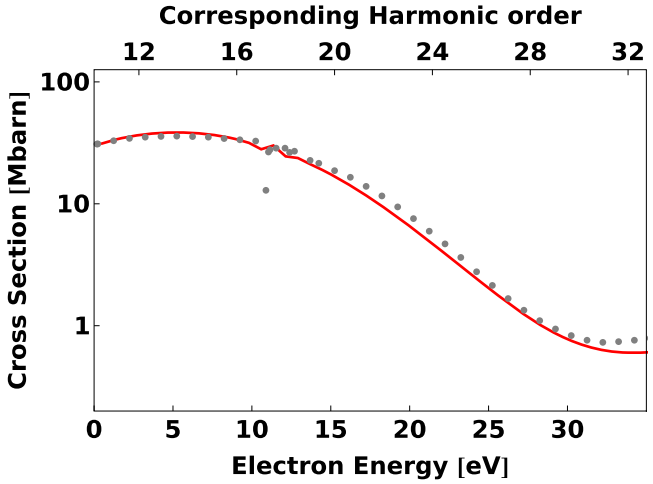

Figure 1. Argon photo-ionization cross section, as a function of electron kinetic energy, calculated within the random phase approximation (RPAE) (cf [20]) compared to experimental results from Samson and Stolte [21]. The upper horizontal axis is marked according to the corresponding absorbed photon energy, given in units of the number of harmonics of an 800 nm laser. The structure just above electron energies of 10 eV is due to resonances bound below the second ionization threshold which are not properly accounted for with RPAE.

approximation we call *DipA2*;

$$\frac{\mathrm{d}P^{DipA2}}{\mathrm{d}\,\mathrm{E}} = k\int \mathrm{d}\Omega_k\ |\boldsymbol{L}(\boldsymbol{k})|^2\ \frac{1}{4\pi}\int \mathrm{d}\Omega_k\ |\boldsymbol{M}(\boldsymbol{k})|^2$$
$$= \frac{(2\pi)^{-3}}{2\alpha\omega_{fi}}\,\sigma^{Ph}\Big|_{\Omega=\omega_{fi}}\int \mathrm{d}\Omega_k\ |\boldsymbol{M}(\boldsymbol{k})|^2. \qquad (8)$$

Both the *DipA* and the *DipA2* will be used below.

2.2. Random phase approximation with exchange

As discussed in connection with equations (6)–(7) above, the factor $\boldsymbol{L}$ can be obtained from the one-photon cross section, σ^{Ph}. Here we have chosen to calculate it within the random phase approximation with exchange (RPAE). The RPAE approximation usually performs well for ionization from rare gas atoms in energy regions where there are no resonances. It allows for channel mixing and polarization of the atom due to the presence of the electromagnetic field. In addition, it accounts for a significant part of the ground state correlation. RPAE gives a good position of the so-called Cooper minimum, and has the attractive property of being gauge independent. Descriptions of the method can be found in [14, 18–20], and here we use the implementation from [19, 20]. In figure 1 the results for the one-photon cross section calculated within the RPAE approximation are compared with experimental data from [21]. As can be seen the agreement is very good in the displayed energy region, with the exception of the resonance(s) just above 10 eV which is not properly accounted for. The energy region shown in figure 1 is the most important for comparison with the experimental data from Heissler *et al* [4], where the XUV pulse is dominated by the 11th to the 16th harmonics of the fundamental laser frequency (cf the upper horizontal scale in figure 1).

2.3. Description of the light-field

Finally we need to specify the light-field. To compare with [4] we build a finite XUV-pulse from the sum of the 11th to the 16th harmonics of the fundamental frequency, ω_0 (here corresponding to $\lambda = 800$ nm). Each harmonic contribution is modeled by a sin-square envelope and with the linear polarization direction given by the vector $\hat{\varepsilon}$:

$$\boldsymbol{F}(t) = \hat{\varepsilon}\sum_{n=11}^{16} F_n \cos\left(n\omega_0(t-t_n) - \phi_n\right)\sin^2\left(\pi(t-t_n)/\tau_n\right). \qquad (9)$$

Each term vanishes outside the time interval $0 < t - t_n < \tau_n$, has an amplitude F_n, a delay t_n and a duration τ_n. For each harmonic the phase $\phi_n = n\omega_0\tau_n/2$ is fixed to obtain a symmetrical pulse with maximum amplitude at the middle of its duration. The lower limit for the obtained focused intensity is in [4] given to $5\cdot 10^{11}$ W cm^{-2}, and here we have varied the values for F_n in accordance with this condition, using peak electric fields ~ 0.003–0.02 au (corresponding to intensities $5\cdot 10^{11} - 10^{13}$ W cm^{-1}). The total duration, τ, of the pulse, defined as the maximum value of $\tau_n + t_n$, has been chosen in order to obtain an electron spectrum resembling that of [4], see section 3.2 below.

3. Results

3.1. Validation of the CV, DipA and DipA2 approximations

In a previous study [16] the accuracy of the CV description was analyzed by comparing it with the time-dependent Schrödinger equation (TDSE) for the ionization of H(1s). The CV results compared generally very well with the TDSE. The parameters that will be considered here, $\hbar\omega \sim 0.5 - 1$ au (1 au ≈ 27.211384 eV), and peak electric fields $\sim 0.003 - 0.02$ au (corresponding to intensities $5\cdot 10^{11} - 10^{13}$ W cm^{-1}), are rather similar to one of the investigated cases (figure 1 in [16]), where the DipA-approximation further reproduced almost exactly the CV ionization spectra in the region where the one-photon process is dominant (lowest electron energy peak), while the lower ATI-peaks show a qualitative agreement, but with an underestimated overall height.

To further check the DipA-approximation for the present study we perform a hydrogen-like calculation with an effective nuclear charge of $Z_{eff} \approx 3.23$ au, which reproduces the correct ionization energy of argon. With this model we calculate both the CV approximation and the DipA-approximation, see the comparison in figure 2. As a starting point we will fix $t_n = 0$, $\tau_n = \tau = 7.8$ fs and $F_n = F_0 = 0.01$ au for all n, but then we will continue to calculate where these parameters are varied in order to investigate the sensitivity to the precise electromagnetic field. Three regions can be distinguished in figure 2: from 0 to 10 eV, 17 to 35 eV and 35 to

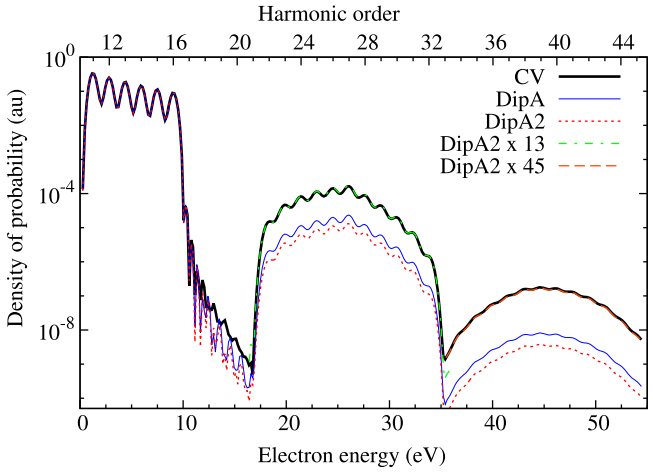

Figure 2. Comparison of CV, DipA and DipA2 spectra for H($3p_0$) ionization due to a coherent XUV-pulse equation (9) with ω_0 corresponding to 800 nm, $F_n = 0.01$ and $\tau = 7.8$ fs. The frequencies vary from $11\omega_0 = 0.63$ to $16\omega_0 = 0.91$ au. An effective charge $Z_{eff} = 3.23$ au was used. The top label indicates the value n such that $E = n\omega_0 - I_p$.

55 eV, corresponding to the process of absorption of one, two and three photons respectively. Comparing the CV, DipA and DipA2 results we note as in [16] that DipA and DipA2 reproduce exactly the CV lowest electron-energy peak, but underestimate the 2nd and 3rd ATI peaks with one and two orders of magnitude respectively. Despite this, the shape of the spectra remains unchanged: when we scale with an arbitrary factor in each region to fit the spectra, the CV results are very well reproduced. Thus, we expect that both DipA and DipA2 should yield reasonable spectra, although lacking the correct relative normalization for the different multi-photon processes.

3.2. Argon spectra

Now we may proceed to the argon calculations where we use the RPAE one-photon cross sections, which account for multi-electronic effects, combined with the expressions in equations (7) or (8) to construct the electron emission spectra due to multi-photon absorption.

First we consider the same XUV-pulse as in the previous section. It is plotted in figure 3(a) with $F_n = 0.01$ au $t_n = 0$ and $\tau = 7.8$ fs. Each of the six terms in equation (9) is plotted with thin (color) lines and the sum of all contributions with a thick (black) line. We can observe that the total pulse behaves like a train of three shorter pulses of ∼1.5 fs.

The frequency domain of this pulse is presented in figure 3(b) together with the DipA spectrum. The six principal peaks of the Fourier transform, corresponding to the six harmonics (11th − 16th of the laser field), are contained in the factor $\boldsymbol{M}$, cf equation (5), and can be recovered if we divide the DipA spectrum by the one-photon cross section. The presence of the Volkov phase in equation (5) is the unique difference between the $\boldsymbol{M}$-factor and the Fourier transform of the pulse. It modifies the higher 'multi-photon' peaks, while the first one is unaltered, and thus the modulus square of the Fourier transform of the pulse can always be recovered from the DipA spectrum in the region of one-photon absorption.

The argon spectrum from the DipA-approximation obtained with the XUV-field in figure 3 is presented in figure 4. We show with dashed (color) lines the ionization spectra from each harmonic separately. The first six peaks are positioned at $E = n\hbar\omega_0 - I_p$ corresponding to the absorption of only one photon of frequency $n\hbar\omega_0$ ($11 \leqslant n \leqslant 16$), where the first ionization potential (I_p) of argon is ∼15.76 eV.

The eleven peaks with energies in the range $(22 - 32)\ \hbar\omega_0$ correspond to the absorption of two photons, $E_{nn'} = (n + n')\hbar\omega_0 - I_p$, where different combinations of n and n' can lead to the same excess energy, thus contributing to the same ATI peak. In figure 4(b) we have plotted this part of the spectra on a linear scale. The figure shows the DipA results for both the H-like model (cf section 3.1 above) and argon. The two spectra show clearly different relative heights of the peaks, indicating a significant sensitivity to the target description. On the other hand, DipA2 and DipA only differ with a global factor. This indicates that the electromagnetic field couples uniformly with electrons ejected at different angles.

The argon spectrum, given by the thick (red) line in figure 4, agrees qualitatively with the experimental result of [4], in particular with the average over several laser shots presented in figure 3(b) of this reference. The pulse duration used in our model, 7.8 fs, has indeed been chosen to maximize the resemblance. As in the average experimental spectra, our model shows a maximum ionization probability in the energy region corresponding to the 25th to 27th harmonics. This is in accordance with the intuitive idea that there is a maximum number of two-photon combinations in this energy region (see figure 2 of [4]).

However, [4] also presents a single shot PE spectrum that shows the opposite behaviour: a minimum in the zone of the 27th harmonic. In order to analyze the sensitivity of the spectra, in the next section we study the results according to different parameters of the XUV-pulse.

3.3. Varying laser pulse parameters

The experimental work [4] includes the PE spectrum for a single laser shot which is quite different from the average of several shots (compare the black line with the red line of figure 3 in this reference). The most significant difference is the minimum in the 26th harmonic instead of a maximum. The question that we want to answer here is what the origin of this minimum is and whether it is possible to reproduce it with our theory. Furthermore, can we determine the laser pulse (intensity, duration and shape) of this shot knowing the PE spectrum?

For this reason, in figures 5 and 6 we present the experimental single shot PE spectrum from [4] (the black line with dots) and our theoretical spectra (filled curve) for different values of the parameters F_n, τ_n and t_n of the laser pulse equation (9) posted in table 1. The left columns present the electric pulses as functions on time. The PE spectra

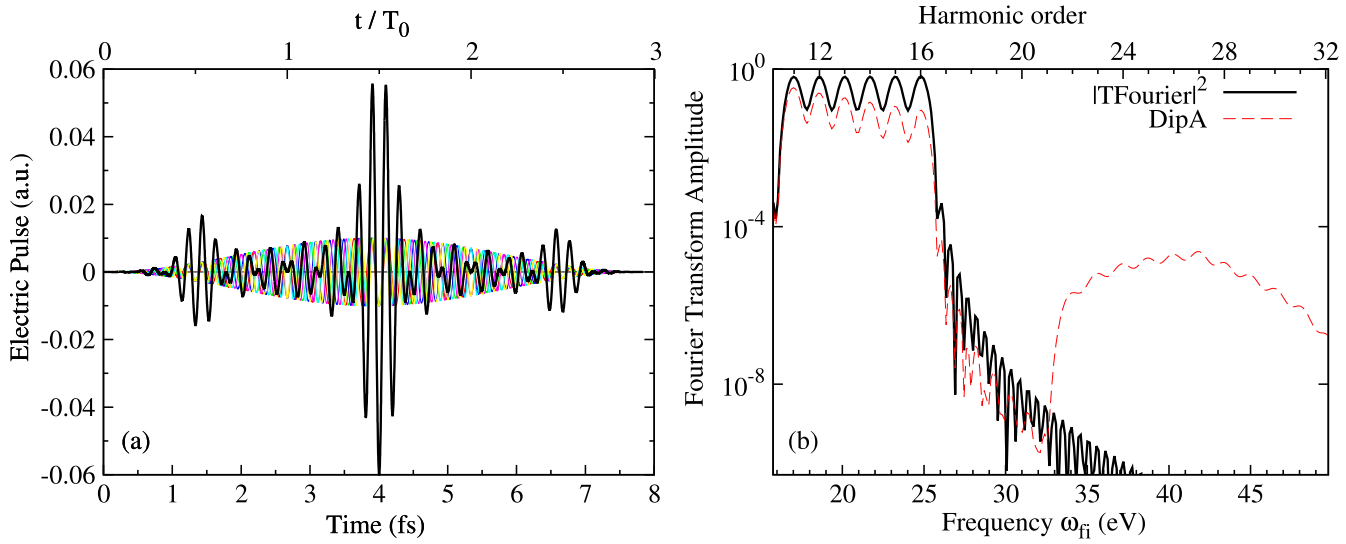

Figure 3. (a) Coherent XUV-pulse equation (9) with $F_n = 0.01$ and $\tau = \tau_n = 7.80$ fs and $t_n = 0$. Here $T_0 = 2\pi/\omega_0$ in the upper horizontal scale is the period of the 800 nm laser field. Thin (color) lines show each harmonic separately. (b) The square modulus of the Fourier transform of the XUV-pulse is shown as a solid line and the DipA spectrum as a dashed line. The ratio of the DipA spectrum and σ^{Ph} equals by construction the first six peaks in the Fourier transform corresponding to the 11th − 16th harmonics of the laser field, cf the upper horizontal axis.

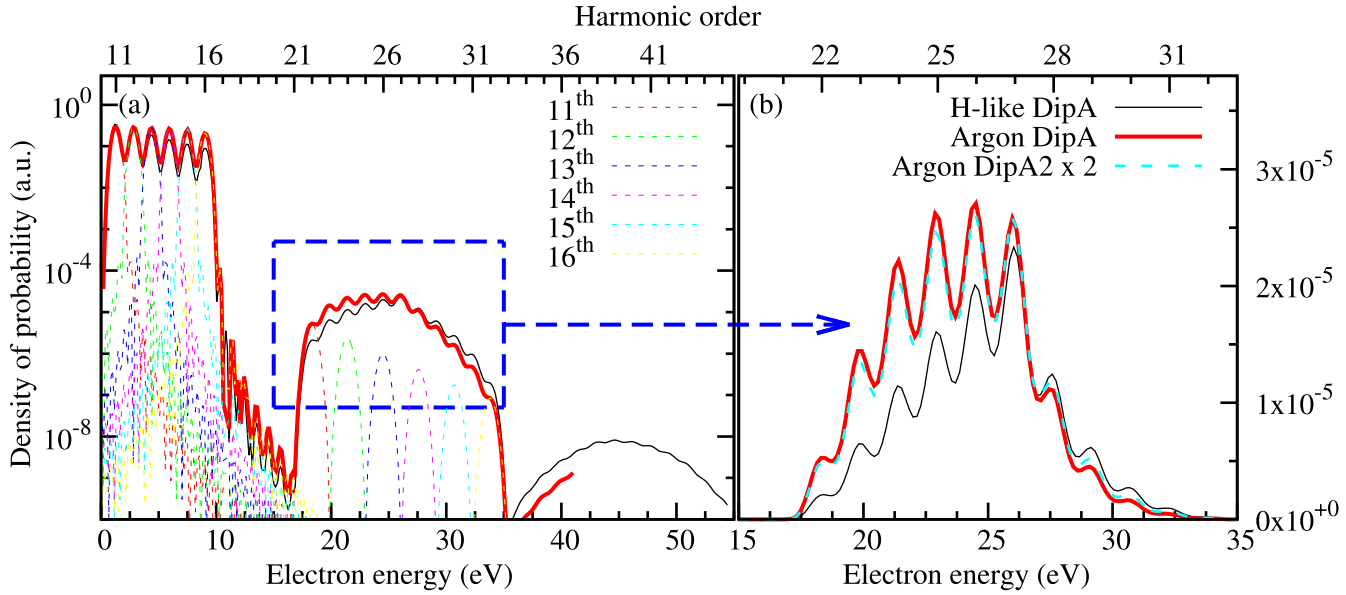

Figure 4. Argon $3p_{m=0}$ ionization spectra as obtained with a 7.8 fs multicolor XUV-pulse. (a) Thin (black) line: H-like, thick (red) line: argon equation (7) and dashed (colors): the contribution of each monochromatic component separately. (b) The zoom of the two-photon absorption region (linear scale). The dashed line (cyan) shows the argon photo electron spectrum as calculated with equation (8) after multiplication by two.

corresponding to these pulses are presented in the center and right columns of these figures. The center (right) figures correspond to the region of single- (two-) photon absorption respectively.

First of all we consider, as in the previous section, a laser pulse with identical parameters for all harmonics (figure 5 (a, b, c) and the first row of table 1). It is the same spectrum shown in figure 4, where we have mentioned that it is qualitatively in agreement with the average shots result, but as we can now see, it disagrees with the single shot measurement. In order to reproduce the height of the experimental single shot spectrum in the low energy zone of the spectra, we adjusted the intensity of each contribution (see second row); and finally, in the third row, we modified the duration τ_n to adjust the width as well. The values of these parameters are shown in the second and third row of table 1. It is clear that by modifying these two variables, F_n and τ_n, it is possible to fit the region of one-photon absorption rather well, i.e. the square modulus of the Fourier transform (as we have discussed before).

We expect then, that the other variables, the delay t_n and ϕ_n, play an important role in the determination of the second

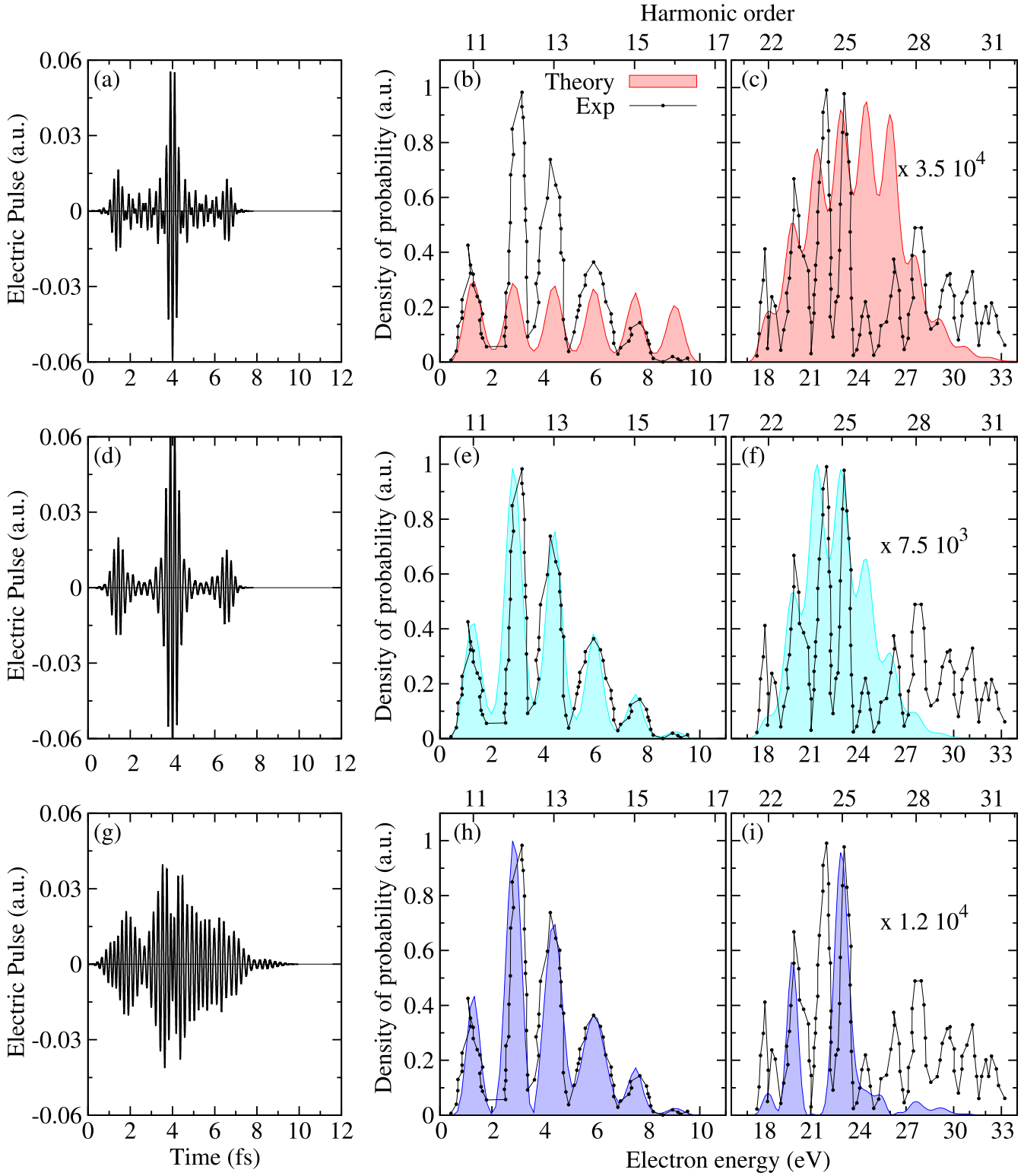

Figure 5. Laser pulse (left column) and PE spectra in the region of one-photon (center column) and two-photon (right column) absorption. Line with dots: experimental spectra from [4]. Filled curve: theoretical result for laser parameters as in table 1. Right column spectra are multiplied by the factor indicated in the graphs.

region of the spectra. However, as we have mentioned before, in this work we fixed the parameter $\phi_n = n\omega_0\tau_n/2$ to achieve the maximum amplitude F_n at time $t = t_n + \tau_n/2$. Hence, the variation of this parameter is intrinsically correlated with the variation of F_n and t_n, and we have decided to keep the phase constant and vary the amplitude and delay independently.

The delay t_n does not influence the one-photon region of the spectrum significantly; in contrast, the two-photon region

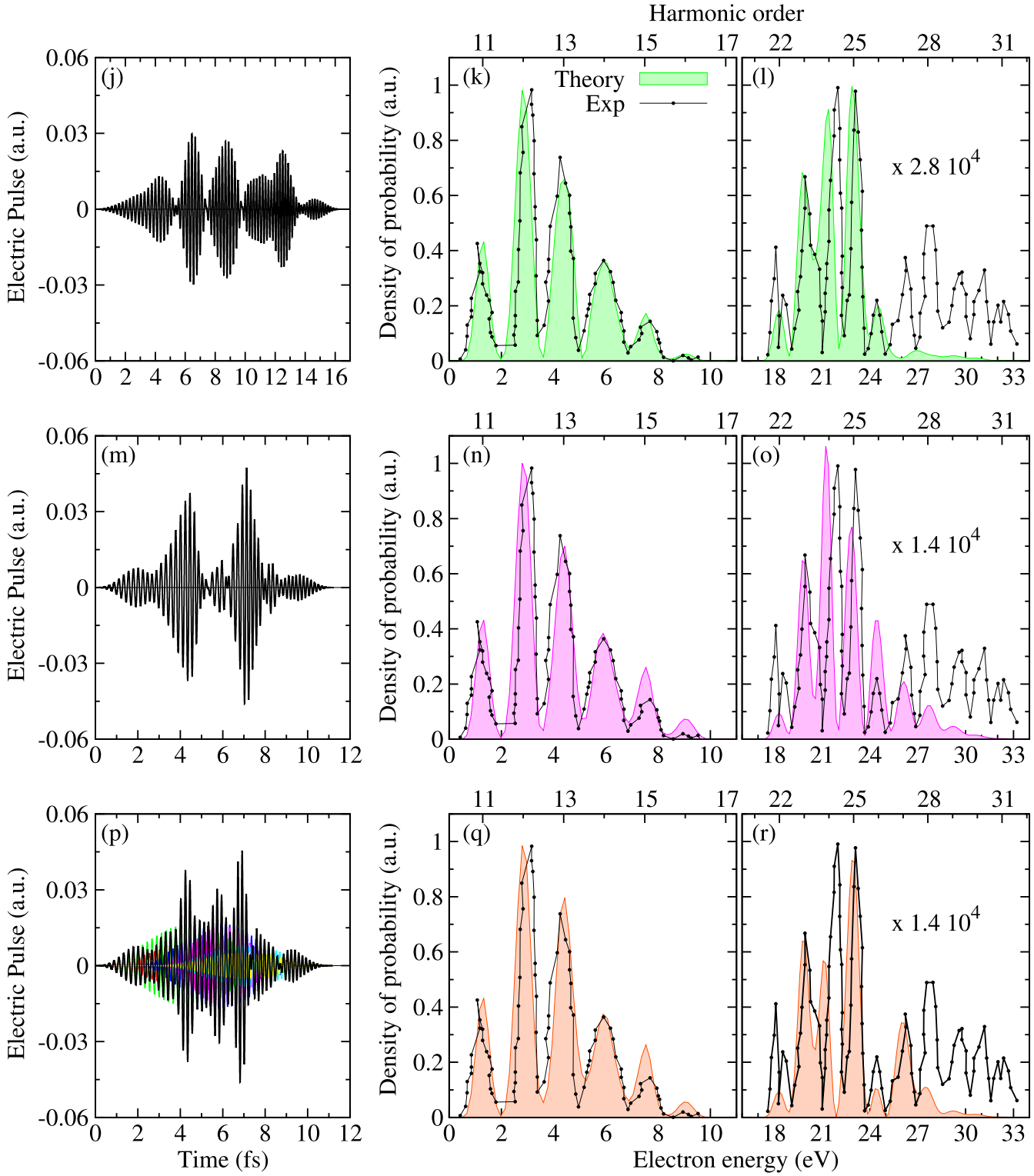

Figure 6. Idem figure 5.

(right column of figures 5 and 6) is very sensitive to this parameter. This fact can easily be understood by considering extreme conditions: a long delay between each harmonic (longer than the duration of each one, for example) does not permit the absorption of two photons of different color simultaneously. This should affect the spectrum considerably since when only the absorption of photons of the same color is considered, the spectrum is greatly reduced (see dashed thin lines in figure 4). On the other hand, if there is no delay, all combinations of two photons are allowed. Thus, the absorption of a pair of photons of different color is very sensitive to the precise value of t_n.

In figure 6, we investigate the effect of a non-zero delay, t_n. Comparing, for example, figure 5(i) with figure 6(l) (see

Table 1. Table of laser parameters. The duration of each harmonic is fixed to enter an integer number of cycles.

figures	amplitude F_n (10^{-2}au)						duration τ_n (fs)						delay t_n (fs)					
	F_{11}	F_{12}	F_{13}	F_{14}	F_{15}	F_{16}	τ_{11}	τ_{12}	τ_{13}	τ_{14}	τ_{15}	τ_{16}	t_{11}	t_{12}	t_{13}	t_{14}	t_{15}	t_{16}
5(a,b,c)	$1\ \forall\ n$						$7.8\ \forall\ n$						$0\ \forall\ n$					
5(d,e,f)	1.20	1.85	1.65	1.20	0.80	0.35	$7.8\ \forall\ n$						$0\ \forall\ n$					
5(g,h,i)	0.94	1.62	1.65	1.56	0.80	0.35	9.9	8.9	7.4	5.9	7.8	7.8	$0\ \forall\ n$					
6(j,k,l)	0.94	1.62	1.65	1.56	0.80	0.35	9.9	8.9	7.4	5.9	7.8	7.8	0	2.7	4.6	8.6	8.6	8.6
6(m,n,o)	0.94	1.62	1.65	1.56	0.99	0.60	9.9	8.9	7.4	5.9	7.8	7.8	0	0	2.4	3.4	3.4	3.4
6(p,q,r)	0.94	1.62	1.65	1.56	0.99	0.60	9.9	8.9	8.0	5.9	8.2	8.2	0	0	1.9	3.0	3.0	3.0

also 3rd and 4th rows of table 1) we see that pulse (g) and (j) give more or less the same one-photon spectra (or square modulus of laser pulse Fourier transform) as graph (h) and (k), but very different two-photon spectra from (i) and (l).

Cases (j, k, l) in figure 6 further reproduce the experimental points well until the 26th peak, but not the 27th to 32nd harmonics. One reason could be the very small contribution of the 15th and 16th harmonics. For that, we increase the values F_{15} and F_{16} and the duration τ_{15} and τ_{16} in (m, n, o) and (p, q, r), see figure 6, in order to increase the peaks corresponding to the 27th to 32nd harmonics. As we can see in graphs (o) and (r), it seems, however, not to be enough. With even higher amplitudes F_{15} and F_{16} the agreement with experimental data in the one-photon region of the spectra will be lost. This suggests that the experimental spectra for the two regions might not be from the same shot. This point is not clearly stated in [4].

The last point we want to discuss is the minimum at 24 eV in the experimental spectrum. One way to reduce the intensity of a certain region in a spectrum is, for example, to isolate a specific harmonic in time. As we have shown in figure 4, when only one color is involved, the absorption probability is reduced by more than one order of magnitude. One possibility is a scenario in which the first two harmonics start simultaneously, a short time before the isolated 13th harmonic, and then the 14th to 16th harmonics are delayed further. This situation is presented in cases (m, n, o) and (p, q, r) in figure 6 and table 1. The delays between the starting time are around 2 fs ($= t_{13} - t_{12}$) and 1 fs ($= t_{14} - t_{13}$). With a subtle variation of parameters we were thus able to reproduce the experimental minimum at the energy value corresponding to the 26th harmonic, see figure 6(r), but the spectrum is then reduced in the region from the 28th to the 32nd harmonics as well.

To summarize, we have varied the laser parameters to try and obtain agreement with single shot experimental data. We have observed that the one-photon region in the PE (i.e. the modulus of the Fourier transform of the pulse) is primarily affected by the duration and amplitude of each harmonic, τ_n and F_n, and is not affected significantly by other parameters. On the other hand, the two-photon region is very sensitive to all laser parameters. In particular, we could not describe the high energy zone of the spectra (27th to 32nd harmonic order). One explanation for this might be that the form of the laser pulse in equation (9) is not suitable; another possibility is that the experimental single-shot PE spectra for one- and two-photon absorption do not correspond to the same shot.

4. Conclusions

We have calculated argon photo-electron spectra using XUV-pulse parameters similar to those used in a recent experiment on two-photon above-threshold ionization.

In the analysis we used approximations of the Coulomb–Volkov approach allowing for a division of the contributions to the spectra into one part that accounts for the bound–continuum transition, including target structure, and one that accounts for the interaction of the light-field with the continuum-electron. Using this approximation we have calculated the argon spectra in the range where the absorption of two photons occurs in particular, accounting for many-body effects as well. The combination of photons of different frequencies results in eleven two-photon absorption peaks that are separated by ω_0. We have observed a variation in the relative intensity of these peaks depending on the description of the target and obtain good qualitative agreement with experimental data, with the average over several laser shots in particular. Furthermore, we have analyzed the PE spectra dependence on the laser parameters and demonstrated a pronounced sensitivity to the particular pulse description in the multi-photon region.

Acknowledgments

This work was undertaken with the support of the FP7-PEOPLE-2010-IRSES, program 269243 DWBQS. EL also acknowledges support from the Swedish Research Council, Grant No. 2012-3668.

References

[1] Krausz F and Ivanov M 2009 *Rev. Mod. Phys.* **81** 163–234
[2] Tsakiris G D 2006 Many and more *New J. Phys.* **8** 19
[3] Nomura Y *et al* 2009 *Nat. Phys.* **5** 124
[4] Heissler P, Tzallas P, Mikhailova J M, Khrennikov K, Waldecker L, Krausz F, Karsch S, Charalambidis D and Tsakiris G D 2012 *New J. Phys.* **14** 043025

[5] Smyth E S, Parker J S and Taylor K T 1998 *Comput. Phys. Commun.* **14** 1
[6] Lagmago Kamta G and Starace A F 2002 *Phys. Rev.* A **65** 053418
[7] Feist J, Nagele S, Pazourek R, Persson E, Schneider B I, Collins L A and Burgdörfer J 2009 *Phys. Rev. Lett.* **103** 063002
[8] Nepstad R, Birkeland T and Førre M 2010 *Phys. Rev.* A **81** 063402
[9] Argenti L and Lindroth E 2010 *Phys. Rev. Lett.* **105** 053002
[10] Argenti L, Pazourek R, Feist J, Nagele S, Liertzer M, Persson E, Burgdörfer J and Lindroth E 2013 *Phys. Rev.* A **87** 053405
[11] Sanz-Vicario J L, Bachau H and Martín F 2006 *Phys. Rev.* A **73** 033410
[12] Milosevic D B, Paulus G G, Bauer D and Becker W 2006 *J. Phys. B: At. Mol. Opt. Phys.* **39** R203
[13] Duchateau G, Cormier E and Gayet R 2002 *Phys. Rev.* A **66** 023412
[14] Amusia M Y 1990 *Atomic Photoeffect* (New York: Plenum)
[15] Della Picca R and Lindroth E 2015 *J. Phys.: Conf. Ser.* **583** 012040
[16] Della Picca R, Fiol J and Fainstein P D 2013 *J. Phys. B: At. Mol. Opt. Phys.* **46** 175603
[17] Bransden B H and Joachain C J 1983 *Physics of Atoms and Molecules* (New York: Wiley)
[18] Mårtensson-Pendrill A M 1985 *J. Physique* (*Paris*) **46** 1949
[19] Dahlström J M, Carette T and Lindroth E 2012 *Phys. Rev.* A **86** 061402(R)
[20] Dahlström J M and Lindroth E 2014 *J. Phys. B: At. Mol. Opt. Phys.* **47** 124012
[21] Samson J A R and Stolte W C 2002 *J. Electron Spectrosc. Relat. Phenom.* **123** 265–76